In *Proceedings of the National Conference on Artificial Intelligence AAAI-93*, 844-49, 1993.

On the qualitative structure of temporally evolving visual motion fields

Richard P. Wildes
SRI David Sarnoff Research Center
Princeton, New Jersey 08543-5300
wildes@sarnoff.com

Abstract

This paper presents a qualitative analysis that relates stable structures in visual motion fields to properties of corresponding three-dimensional environments. Such an analysis is fundamental in the development of methods for recovering useful information from dynamic visual data without the need for highly accurate and precise sensing. Methodologically, the techniques of singularity theory are used to describe the mapping from image space to velocity space and to relate this mapping to the three-dimensional environment. The specific results of this paper address situations where an optical sensor is undergoing pure rotational or pure translational motion through its environment. For the case of pure rotational motion it is shown that the qualitative structure of visual motion provides information about the axes and relative magnitudes of rotation. For the case of pure translational motion it is shown that the qualitative structure of visual motion provides information about the shape and orientation of viewed surfaces as well as information about the translation itself. Further, the temporal evolution of the visual motion field is described. These results suggest that valuable information regarding three-dimensional environmental structure and motion can be recovered from qualitative consideration of visual motion fields.

Introduction

The visual motion field is the image projection of an environment that is moving relative to an optical sensor. As such, this field is a potentially rich source of information about the environment as well as the relative motion between the environment and sensor. In response to this possibility, this paper concentrates on developing an understanding of the qualitative properties of the motion field and of its relationship to an impinging visual world. In essence, this understanding is based on an analysis of stable structures in temporally evolving visual motion fields. Structural stability refers to properties that persist independently of minor perturbations to the visual motion field. In practice, this is of considerable importance as the visual motion field is not directly recoverable from optical data. Instead, only a near relative, the optical flow, the apparent motion of brightness patterns is recoverable (Horn 1986). Further, even obtaining good estimates of the optical flow has proven to be fraught with numerical difficulties. Happily, by concentrating on structurally stable properties of the visual motion field one has a rich source of information without reliance on highly accurate and precise recovery of the flow.

A great deal of research has focused on the interpretation of visual motion; general reviews are available (e.g., Hildreth & Koch 1987). Most relevant for current purposes are other qualitative analyses: The visual motion field has been decomposed into primitive fields to expose its underlying structure (Hoffman 1966; Koenderink & van Doorn 1975). The significance of stationary points has been addressed (Verri *et al.* 1989). Issues of uniqueness have received attention (Carlsson 1988). Interestingly, the bulk of these studies have couched their analyses in the language of dynamical systems theory (Hirsch & Smale 1974).

In contrast to prior work, this paper employs singularity theory (Arnold 1991) and its application to vector fields (Thorndike *et al.* 1978) to uncover and study information rich yet structurally stable properties of the flow. Presently, consideration is restricted to cases of visual motion due to either pure rotational or pure translational 3D motion. Specific contributions of this research include: First, for pure rotational 3D motion, it is shown that in principle qualitative considerations allow for the recovery of the axis of angular rotation, the direction of rotation and the ratio of the magnitudes of angular and radial rotation. Second, for pure translational 3D motion, it is shown that in principle qualitative considerations allow for the recovery of a description of viewed surface shape, information about the direction of viewed surface gradient and information about the direction of angular translation. Third, the temporal evolution of the visual motion field is described in terms of smooth changes and a set of three events marking more abrupt transitions.

Preliminary developments

For current purposes, it is useful to conceptualize of the visual motion field as a vector mapping, $\mathbf{f}$, assigning to each point $\mathbf{p} = (x, y)$ in the source space, $\mathcal{P}$, of image positions a single velocity vector $\mathbf{v} = (u, v)$ in the target space, $\mathcal{V}$, of image velocities $\mathbf{f} : \mathcal{P} \rightarrow \mathcal{V}$ or $\mathbf{v} = \mathbf{f}(\mathbf{p})$. It also is useful to introduce the Jacobian of the velocity mapping

$$\mathrm{J} = \begin{pmatrix} \frac{\partial u}{\partial x} & \frac{\partial u}{\partial y} \\ \frac{\partial v}{\partial x} & \frac{\partial v}{\partial y} \end{pmatrix}. \qquad (1)$$

Singular points of the mapping $\mathbf{f} : \mathcal{P} \rightarrow \mathcal{V}$ are defined to be points $\mathbf{p}$ where $\det(\mathrm{J}) = 0$. Points that are not singular are said to be regular. In the plane, these distinctions have simple geometric interpretations: A small circle centered about a regular point in $\mathcal{P}$ will be mapped to an ellipse in $\mathcal{V}$. Correspondingly, at each of these points there is a direction, $\mathbf{a}$, that leads to the maximal change in length as the circle deforms into the ellipse. The magnitude of the determinant, $\det(\mathrm{J})$, gives the ratio of corresponding areas in $\mathcal{V}$ and $\mathcal{P}$. However, at singular points the image ellipse degenerates into a line segment; the ratio of areas is zero, i.e., $\mathrm{Ja} = 0$.

The structurally stable singularities of any mapping $\mathbf{f} : \Re^2 \rightarrow \Re^2$ form lines (Whitney 1955). Structurally stable properties are of interest as they are the properties that are robust to slight perturbations of the mapping, e.g., as due to varying observation conditions; for a formal definition of structural stability see (Golubitsky & Guillemin 1973). In the source space, $\mathcal{P}$, the structurally stable lines of singularity are smooth and are referred to as fold-lines. In the target space, $\mathcal{V}$, the images of the fold lines also are lines and are called folds. However, along the fold-lines are special points, called cusps, distinguished by tangency with the $\mathbf{a}$-trajectories. The image of these points in $\mathcal{V}$ appear as cusps along the folds. Since fold-lines and folds as well as cusp points and cusps form stable structures in a 2D to 2D mapping, they will serve as the focus in the following structural analysis of the visual motion field. Figure 1 illustrates the geometry of folds and cusps in the velocity mapping.

Structural analysis of visual motion

Define a Cartesian coordinate system at the center of an optical sensor with the Z-axis pointing along the optical axis. Under perspective projection a 3D point $\mathbf{P} = (X, Y, Z)$ is mapped to an image point $\mathbf{p} = (\frac{X}{Z}, \frac{Y}{Z}) = (x, y)$, where appropriate scaling is taken so that the focal length is unity. Let visual motion derive from a sensor moving through a static environment. (Alternatively, it could be assumed that a fixed sensor observes a dynamic environment.) Take the sensor's translational velocity as $\mathbf{T} = (t_x, t_y, t_z)$, while its rotational velocity is $\Omega = (\omega_x, \omega_y, \omega_z)$. Then, the equations of rigid body motion and perspective

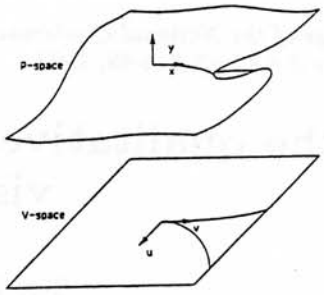

Figure 1: The velocity mapping $\mathbf{f}$ can be thought of as stretching and bending the source space of image positions, $\mathcal{P}$, in three dimensions and then projecting it into the target space of image velocities, $\mathcal{V}$. $\mathcal{P}$ is folded along fold-lines that project to folds. Cusp-points correspond to pleats along the fold-lines that project to cusps.

projection, allow the image velocity, $\mathbf{v} = (u, v)$, of an environmental point, $\mathbf{P}$, to be written as

$$\begin{aligned} u &= \tfrac{1}{Z}(xt_z - t_x) + xy\omega_x - (x^2 + 1)\omega_y + y\omega_z \\ v &= \tfrac{1}{Z}(yt_z - t_y) + (y^2 + 1)\omega_x - xy\omega_y - x\omega_z \end{aligned} \qquad (2)$$

(Horn 1986). The visual motion field is an array of velocities $\mathbf{v}$, for an imaged 3D environment. Correspondingly, the terms of the velocity Jacobian (1) can be expanded as

$$\begin{aligned} \tfrac{\partial u}{\partial x} &= \left(\tfrac{\partial}{\partial x}\tfrac{1}{Z}\right)(xt_z - t_x) + \tfrac{t_z}{Z} + y\omega_x - 2\omega_y x \\ \tfrac{\partial u}{\partial y} &= \left(\tfrac{\partial}{\partial y}\tfrac{1}{Z}\right)(xt_z - t_x) + x\omega_x + \omega_z \\ \tfrac{\partial v}{\partial x} &= \left(\tfrac{\partial}{\partial x}\tfrac{1}{Z}\right)(yt_z - t_y) - \omega_y y - \omega_z \\ \tfrac{\partial v}{\partial y} &= \left(\tfrac{\partial}{\partial y}\tfrac{1}{Z}\right)(yt_z - t_y) + \tfrac{t_z}{Z} + 2\omega_x y - \omega_y x \end{aligned} \qquad (3)$$

Now, consider purely rotational 3D motion. The governing conditions are $\mathbf{T} = \mathbf{0}$, while $\Omega = (\omega_x, \omega_y, \omega_z)$. In these situations the visual motion field specializes to

$$\begin{aligned} u &= \omega_x xy - \omega_y(x^2 + 1) + \omega_z y \\ v &= \omega_x(y^2 + 1) - \omega_y xy - \omega_z x \end{aligned} \qquad (4)$$

An illustration of a visual motion field due to 3D rotation is shown in the left side of Figure 2. Under pure 3D rotation, the condition for singularity, $\det(\mathrm{J}) = 0$, dictates that the expression

$$2\omega_y^2 x^2 + 2\omega_x^2 y^2 - 4\omega_x\omega_y xy + \omega_x\omega_z x + \omega_y\omega_z y + \omega_z^2 \qquad (5)$$

evaluates to zero. To understand the form of the singularity in the source space, $\mathcal{P}$, consider the discriminant (Korn & Korn 1968) of the condition (5) viewed as a conic section,

$$(-4\omega_x\omega_y)^2 - 4(2\omega_y^2)(2\omega_x^2). \qquad (6)$$

Since the discriminant (6) is identically equal to zero, the singular points are manifest in $\mathcal{P}$ as a parabola. This parabola describes the fold line for the case of pure rotational 3D motion.

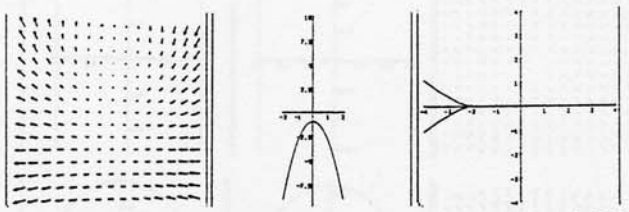

Figure 2: A visual motion field for rotation about the Z and Y axes (left). The fold-lines in the source space, $\mathcal{P}$, of image positions (middle). The corresponding folds with a cusp in the target space, $\mathcal{V}$, of image velocities (right).

In order to facilitate further analysis, a new coordinate system, (x', y') is now adopted so that the parabola shaped fold-line is symmetric about the y'-axis. Consideration of the related equations for the rotation of coordinate axes shows that the y'-axis is parallel to the direction $\frac{(\omega_x,\omega_y)}{\|(\omega_x,\omega_y)\|}$, i.e., the direction of the angular component of 3D rotation. Therefore, in the (x', y') coordinate system 3D rotation is given as $\Omega' = (\omega'_x, \omega'_y, \omega'_z) = (0, (\omega_x^2 + \omega_y^2)^{\frac{1}{2}}, \omega_z)$. The form of the fold-line now can be given as

$$y' = -2\frac{\omega'_y}{\omega'_z}x'^2 - \frac{\omega'_z}{\omega'_y}. \tag{7}$$

From the equation for the fold-line in the (x', y') coordinate system (7) a number of observations are immediate: First, this parabola intercepts the y'-axis at $-\frac{\omega'_z}{\omega'_y}$, the ratio of radial to angular components of 3D rotation. Second, by computing the derivative with respect to x it is seen that the parabola opens at the rate $-4\frac{\omega'_y}{\omega'_z}x$, $4x'$ times the inverse of the previous ratio. Third, given the agreement in the signs of these two ratios, the parabola always opens away from the origin. An example fold-line parabola is illustrated in the middle of Figure 2.

To study the locus of singularities in the target space, $\mathcal{V}'$, the equation describing the fold-line in the source space, $\mathcal{P}'$, (7) can be substituted into the equations of the visual motion field (4) to yield

$$(u', v') = \left(-3\omega'_y x'^2 - \frac{\omega'^2_y + \omega'^2_z}{\omega'_y}, \frac{\omega'^2_y}{\omega'_z}x'^3\right). \tag{8}$$

This set of equations can be taken as a parametric representation of the fold in $\mathcal{V}'$ with parameter x'. This curve intercepts the u'-axis at $-\frac{\omega'^2_y+\omega'^2_z}{\omega'_y}$, the negative of the ratio of the squared magnitude of rotational motion to the angular component of rotational motion. As x' differs from zero the curve branches out symmetrically from its u'-intercept, leaving a cusp in its wake. The rate at which the fold opens can be determined by (implicitly) computing the derivative $\frac{dv'}{du'} = -\frac{\omega'_y}{\omega'_z}x'$ to see that the rate of opening (as a function of x') is determined by minus the ratio of angular to radial rotation, $-\frac{\omega'_y}{\omega'_z}$. An illustrative example fold with cusp is shown on the right side of Figure 2.

At this point it is useful to review by noting the ways that the singularities of the velocity mapping could be used to make inferences about 3D rotational motion: First, the appearance of the fold-lines as a parabola with a single cusp-point could be taken as a signature indicative of rotational 3D motion. Second, the axis of angular rotation can be recovered as the axis of symmetry of the fold-line parabola. Third, the distance of the parabola from the origin as well as the rate of opening of the parabolic fold-line and cusped fold are all directly indicative of the relative magnitude of angular and radial rotations. Finally, notice that the singularities say nothing about 3D environmental structure. This reflects the fact that instantaneous visual motion due to purely rotational 3D motion is independent of environmental layout.

Next, consider purely translational 3D motion. The governing conditions are $\mathbf{T} = (t_x, t_y, t_z)$ while $\Omega = 0$. Correspondingly, the visual motion field specializes to

$$(u, v) = \left(\frac{1}{Z}(xt_z - t_x), \frac{1}{Z}(yt_z - t_y)\right). \tag{9}$$

Illustrations of three different visual motion fields due to 3D translation are shown in the first column of Figure 3. Under pure 3D translation, the condition for singularity, $\det(\mathbf{J}) = 0$, dictates that the expression

$$\frac{t_z}{Z}\left(\left(\frac{\partial}{\partial x}\frac{1}{Z}\right)(xt_z - t_x) + \left(\frac{\partial}{\partial y}\frac{1}{Z}\right)(yt_z - t_y) + \frac{t_z}{Z}\right) \tag{10}$$

evaluates to zero.

The translation-based singularity equation (10) involves the translation as well as the shape and pose of a surface of regard. To understand this matter consider a surface described at each point by its local tangent plane, then $n_x X + n_y Y + n_z Z = d$, where the (n_x, n_y, n_z) are normals at points on the surface (X, Y, Z). In this case, $\left(\frac{\partial}{\partial x}, \frac{\partial}{\partial y}\right) \cdot \frac{1}{Z} = \frac{(n_x,n_y)}{Z(n_x x+n_y y+n_z)}$. Substitution into (10) then yields

$$(n_x, n_y, n_z) \cdot \left(2x - \frac{t_x}{t_z}, 2y - \frac{t_y}{t_z}, 1\right) = 0.$$

This expression shows that the singularity condition holds when the local surface normal is orthogonal to

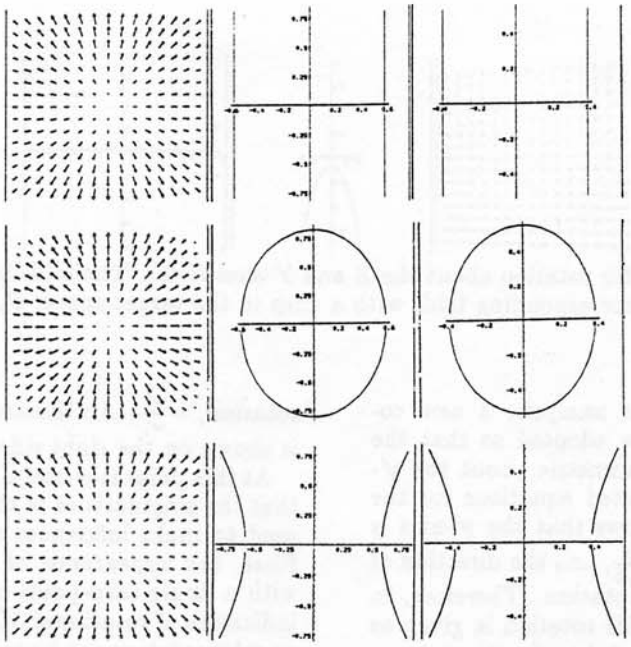

Figure 3: The left column shows visual motion fields for an observer approaching parabolic (top), elliptic (middle) and hyperbolic (bottom) surfaces. The middle column shows the fold-lines in the source space, $\mathcal{P}$, of image positions. The right column shows the folds in the target space, $\mathcal{V}$, of image velocities.

the view direction scaled by two and displaced by the focus of expansion, $t_z^{-1}(t_x, t_y)$; the locus of singularity is indicative of translation, surface shape and pose.

It is illustrative to consider in detail a particular set of examples: Let a surface be represented as a Monge patch, $(X, Y, Z(X, Y))$ with $Z(X, Y) = \frac{1}{2}\kappa_1 X^2 + \frac{1}{2}\kappa_2 Y^2 + \kappa_3 XY + pX + qY + r$ so that $\frac{1}{Z} = \frac{1-px-qy}{r} - \kappa_3 xy - \frac{1}{2}\kappa_1 x^2 - \frac{1}{2}\kappa_2 y^2$, through second-order. When this surface model is made use of in the singularity condition (10) it is found that the locus of singularities in the source space, $\mathcal{P}$, is a quartic in x and y that can be written as the product of two conic sections. However, one of these conic sections corresponds to a degenerate situation where the underlying 3D surface recedes to infinity. Along this contour all the velocities map to a single point, $(0, 0)$. Consequently, subsequent attention will be restricted to the other conic section. To study this curve, it is convenient to immediately adopt a new coordinate system, (x', y'), by rotating the axes so as to eliminate the cross terms in xy. Following this operation, the contour can be written as

$$\begin{aligned} &3\kappa_x r t_z x'^2 + 3\kappa_y r t_z y'^2 + 2(2p' t_z - \kappa_x r t'_x)x \\ &+2(2q' t_z - \kappa_y r t'_y)y' - 2(p' t'_x + q' t'_y + tz) = 0 \end{aligned} \quad (11)$$

where it turns out that κ_x and κ_y are given by diagonalization of the coefficients of the quadratic terms in the Monge patch representation of the surface. As a point of departure on understanding the equation describing the singular points (11) suppose that there is no angular component to translation, i.e., $t'_x = t'_y = 0$, and that the surface gradient vanishes at the origin, i.e., $p' = q' = 0$. Also, for ease of notation, primes will be dropped for the rest of this section of the paper; the fact that all calculations are being performed in the (x', y') coordinate system will be implicit. Under these conditions, equation (11) evaluates to

$$\kappa_x x^2 + \kappa_y y^2 = \frac{2}{3r}. \quad (12)$$

Consideration of this simplified singularity condition (12) shows that it describes an origin centered conic section that is: an ellipse if $sgn(\kappa_x) = sgn(\kappa_y)$, a hyperbola if $sgn(\kappa_x) = -sgn(\kappa_y)$ or parallel straight lines if $\kappa_x = 0$ or $\kappa_y = 0$, i.e., the curves are indicative of Dupin's Indicatrix for the underlying 3D surface Z. Also, the major axis of the conic section is along the x-axis if $\|\kappa_x\| < \|\kappa_y\|$ or along the y-axis if $\|\kappa_x\| > \|\kappa_y\|$. The second column of Figure 3 shows representative examples.

What conclusions can be reached about the form of the fold-lines under less restricted conditions? First, suppose that the restriction against angular translation is removed, i.e., $\mathbf{T} = (t_x, t_y, t_z)$. In this case, the form of the fold-line (12) becomes

$$\kappa_x \left(x - \frac{t_x}{3t_z}\right)^2 + \kappa_y \left(x - \frac{t_y}{3t_z}\right)^2 = \frac{18t_z^3 + t_x^2 + t_y^2}{27 r t_z^3}.$$

In words, the addition of angular motion does not change the qualitative shape of the curve. However,

the size is adjusted and the center moves along the axis of angular translation. Second, suppose that the surface gradient is no longer required to vanish at the origin. In this case, the fold-line equation can be written as

$$\kappa_x \left(x + \tfrac{2p}{3\kappa_x r}\right)^2 + \kappa_y \left(y + \tfrac{2q}{3\kappa_y r}\right)^2 = \tfrac{2}{3r}\left(1 + \tfrac{2}{9r^2 t_z}\left(\left(\tfrac{p}{\kappa_x}\right)^2 + \left(\tfrac{q}{\kappa_y}\right)^2\right)\right).$$

This equation shows that a surface gradient also does not change the qualitative shape of the fold-lines, although the size is altered. The center of the curve again moves in the direction specified by the surface gradient, but as weighted by the surface curvatures κ_x and κ_y. Finally, suppose that both angular translation and non-vanishing gradient are both allowed. In this case, the equation of the fold-line can be written as

$$\kappa_x \left(x + \tfrac{2p}{3\kappa_x r} - \tfrac{t_x}{3t_z}\right)^2 + \kappa_y \left(x + \tfrac{2q}{3\kappa_y r} - \tfrac{t_y}{3t_z}\right)^2 = \tfrac{1}{3rt_z} \times \left(2(pt_x + qt_y + t_z) + \left(\tfrac{pt_z - r\kappa_x t_x}{3r\kappa_x r t_z}\right)^2 + \left(\tfrac{qt_z - r\kappa_y t_y}{3r\kappa_y r t_z}\right)^2\right)$$

As with the other cases, it is seen that the qualitative shape of the contour remains the same. However, now the contour's center is displaced to a point that is the vector sum of the centers for angular translation and non-vanishing gradient.

To study the locus of singularities in the target space, $\mathcal{V}$, begin by again considering the restricted situation where there is no angular translation and the surface gradient vanishes at the image origin. In this case, the corresponding equation describing the fold-line in the source space, $\mathcal{P}$, (12) can be substituted into the equations of the translational visual motion field (9). This operation yields

$$(u, v) = \left(\frac{2x}{3r}, \frac{2\left(\frac{2}{r} - 3\kappa_x x^2\right)^{\frac{1}{2}}}{r(27\kappa_y)^{\frac{1}{2}}}\right). \qquad (13)$$

This set of equations can be taken as a parametric representation of the velocity with parameter x. The shape of the corresponding fold in the target space is a parabola, ellipse of hyperbola depending on the curvature terms, κ_x and κ_y, in exactly the same way as did the fold-lines in the source space; the folds are indicative of Dupin's Indicatrix as were the fold-lines. Three examples of folds are shown in the third column of Figure 3. As in the source space, the addition of angular translation and surface gradient causes the fold conics to drift in position. However, unlike the fold-lines the folds slowly deform as they drift toward the target space periphery.

Again, it is useful to review by explicitly noting several ways that the singularities of the visual motion field can be used to interpret 3D translational motion: First, the shape of the fold-lines are indicative of the qualitative 3D surface shape. For the particular case of quadratic surface patches, the fold-lines form an ellipse, hyperbola or a pair of parallel straight lines according to whether the surface is locally elliptic, hyperbolic or parabolic in shape. This same signature is apparent in the corresponding folds in the target space; however, here they can be deformed by angular translation and surface gradient. Second, the major and minor axes of the surface can be recovered from the corresponding fold-line conic section major and minor axes. Third, the directions of angular translation and surface gradient are constrained by the off-set of the fold-lines from the image origin.

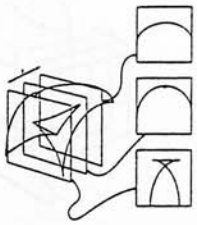

Figure 4: The swallowtail singularity describes the condition when a fold sheet and rib intersect. The swallowtail event occurs when a τ slice contains this type of intersection.

Temporal evolution

In general, visual motion fields evolve in time. Correspondingly, the patterns of the singular points, the folds and cusps, vary with time. More precisely, consider a family of flows, $\{f^t : \mathcal{P} \rightarrow \mathcal{V}\}, -\infty < \sqcup < \infty$. parameterized by t, time. t can be thought of as assigning a particular time to each of the mappings in a given series. Another way of looking at matters is given by taking the family of functions f^t in tandem to define a single function $\mathrm{g} : \Re^3 \rightarrow \Re^3$ i.e., $\mathrm{g} : (x, y, t) \rightarrow (u, v, \tau)$ with the form $(u, v, \tau) = (u(x, y, t), v(x, y, t), t)$. The velocity map at any given time now corresponds to a τ slice. In the (u, v, τ)-space, the folds define surfaces called fold sheets; while, the cusps define lines in those surfaces called ribs. Additionally, a third structure of interest now presents itself, the swallowtail. A swallowtail occurs when a fold sheet and a rib intersect. The canonical form for the swallowtail singularity is

$$(u, v, \tau) = (x^4 + x^2 y + xt, y, t). \qquad (14)$$

Figure 4 illustrates the associated geometry. Of all elementary singularities, only three, the fold, cusp and swallowtail are stable with respect to general perturbations to the time dependent flow (Golubitsky & Guillemin 1973).

Typically, the stable structures of the visual motion field evolve smoothly in time. Reference to the previous section's discussion reveals much of what can be expected. For pure rotational 3D motion: As the direction of angular rotation changes, the orientation of the

Figure 5: The lips (left) and beak to beak (right) events can occur when a τ slice is tangent to a rib.

fold-line parabola in the source space also changes as does the corresponding fold in the target space. As the ratio of angular to radial rotation changes, the fold-line parabola opens and closes and moves toward and away from the origin. Corresponding changes take place with the rate of opening of the two arms of the fold and the distance of the cusp from the origin. As time passes the fold-line and fold sweep out surfaces; the cusp creases the fold sheet with a rib. For pure translational 3D motion: As the observer moves toward or away from a surface of regard the fold-lines and folds expand and contract, without changing their characteristic shape. With angular translation the contours drift in spatial position. Again, surfaces are traced by the smooth evolution of the fold-lines and folds.

In addition to the smooth evolution of the singularities in time more abrupt change can occur. In particular, there are special points along the ribs, called events, that demark more abrupt change and that determine the overall temporal evolution. Strikingly, there are only three distinct types of events for concern in the analysis of vector fields (Thorndike *et al.* 1978). The first of these events is associated with the swallowtail singularity (14). This event occurs when a τ slice contains an intersection of a fold sheet with a rib, see Figure 4. Two additional types of events can occur when a τ slice is tangent to a curved rib: (i) In the lips event an initially structureless region becomes tangent to a rib and subsequently gives rise to a doubly cusped region. (ii) In the beak to beak event two target space regions lose their identity as the event is passed. Lips and beak to beak events are described by

$$(u, v, \tau) = (x^3 \pm xy^2 + xt, y, t),$$

respectively. Figure 5 illustrates these events.

Summary

Qualitative consideration of a visual motion field yields information about the 3D geometry and motion of an impinging environment. In this paper attention has focused on cases where an optical sensor undergoes pure rotation or pure translation. For rotation, information is available about the axes and relative magnitudes of angular and radial rotation. For translation, information is available about the shape and orientation of visible surfaces as well as about the translation itself. In either case, the structure of the flow typically evolves smoothly in time. However, on occasion discrete events occur that add greater richness to the structure.

References

Arnold, V. I. 1991. *The Theory of Singularities and Its Applications.* Cambridge University Press, NY, NY.

Carlsson, S. 1988. Information in the geometric structure of retinal flow fields. In *Proceedings of the International Conference on Computer Vision.* 629–633.

Golubitsky, M. and Guillemin, V. 1973. *Stable Mappings and their Singularities.* Springer, NY, NY.

Hildreth, E. C. and Koch, C. 1987. The analysis of visual motion: From computational theory to neuronal mechanisms. *Annual Review of Neuroscience.*

Hirsch, M. W. and Smale, S. 1974. *Differential equations, dynamical systems and linear algebra.* Academic Press, NY, NY.

Hoffman, W. C. 1966. Lie group theory of visual perception. *Journal of Mathematical Psychology* 3:65–165.

Horn, B. K. P. 1986. *Robot Vision.* MIT Press, Cambridge, MA.

Koenderink, J. J. and van Doorn, A. J. 1975. Invariant properties of the motion parallax field due to the movement of rigid bodies relative an observer. *Optica Acta* 22:717–723.

Korn, G. A. and Korn, T. M., editors 1968. *Mathematical Handbook for Scientists and Engineers, Second Edition.* McGraw-Hill, NY, NY.

Thorndike, A. S.; Cooley, C. R.; and Nye, J. F. 1978. The structure and evolution of flow fields and other vector fields. *Journal of Physics A: Mathematical and General* 11(8):1455–1490.

Verri, A.; Girosi, F.; and Torre, V. 1989. Mathematical properties of the two-dimensional motion field: From singular points to motion parameters. *Journal of the Optical Society of America A* 6(5):698–712.

Whitney, H. 1955. On singularities of mappings of euclidean spaces. i. mappings of the plane into the plane. *Annals of Mathematics* 62(3):374–410.